Journal of Thermal Analysis and Calorimetry, Vol. 93 (2008) 3, 677–687

APPLICATION OF THERMAL ANALYSIS METHODS FOR CHARACTERIZATION OF POLYMER/MONTMORILLONITE NANOCOMPOSITES

*Agnieszka Leszczynska and Krzysztof Pielichowski**

Department of Chemistry and Technology of Polymers, Cracow University of Technology, ul. Warszawska 24, 31-155 Cracow, Poland

Thermal analysis is a useful tool for investigating the properties of polymer/clay nanocomposites and mechanisms of improvement of thermal properties. This review work presents examples of applications of differential scanning calorimetry (DSC), modulated temperature differential scanning calorimetry (MT-DSC), dynamic mechanical thermal analysis (DMA), thermal mechanical analysis (TMA), thermogravimeric analysis (TG) and thermoanalytical methods i.e. TG coupled with Fourier transformation infrared spectroscopy (TG-FTIR) and mass spectroscopy (TG-MS) in characterization of nanocomposite materials. Complex behavior of different polymeric matrices upon modification with montmorillonite is briefly discussed.

Keywords: *DMA, DSC, montmorillonite, polymer nanocomposites, TG, thermal analysis, TMA*

Introduction

During the last decade there has been steadily increasing interest in the field of polymer/clay nanocomposites since the modification of polymer matrix with small amounts of nanoparticles proved to be effective in enhancing the mechanical, thermal, fire retardant, barrier and optical properties of a variety of polymers. Thermal analysis methods were widely applied to characterize the thermal behavior of polymeric nanomaterials. The rich bibliography on polymer/clay nanocomposites shows that the effect of montmorillonite (MMT) on thermal properties of polymer is complex and many factors contribute to the enhancement, such as MMT dispersion, the strength of inter-facial interactions, catalytic effects induced by organomodifier and/or montmorillonite itself, type of polymer matrix, preparation method, etc. However, this work is not intended to be a comprehensive review on the thermal properties of polymeric hybrid materials containing layered silicates, but it illustrates the versatile applications of TA methods in the emerging field of polymer nanomaterials' research.

Thermal analysis methods

Differential scanning calorimetry

Differential scanning calorimetry (DSC) has been widely applied in investigations of numerous phenomena occurring during thermal treatment of organoclays and polymer-clay nanocomposites, involving melting, crystallization, curing and glass transition.

In a work of Tian and Tagaya DSC method was used to investigate the influence of preparation route of nanocomposite material on polymer morphology. The melting enthalpy of poly(lactic acid)/montmorillonite (PLA/MMT) nanocomposites changed with an increase of nanoadditive content, depending on the method of nanocomposite preparation [1]. The changes of melting enthalpy, ΔH, of the PLA/MMT system prepared by the melt extrusion were considerably higher than those obtained by solvent dissolution method, Fig. 1. It was considered that the binding force between PLA and inorganic compound in the composite prepared by melt extrusion method was higher than in those prepared by solvent dissolution method.

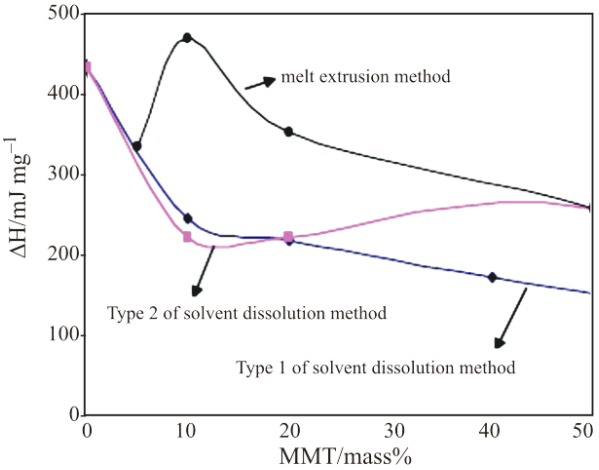

Fig. 1 The melting enthalpy, ΔH, of the PLA/MMT composites prepared by the melt extrusion and solvent dissolution methods [1]

* Author for correspondence: kpielich@riad.pk.edu.pl

1388–6150/$20.00

Akadémiai Kiadó, Budapest, Hungary
Springer, Dordrecht, The Netherlands

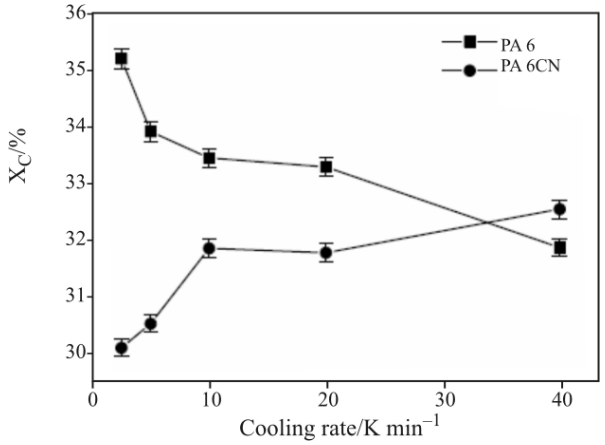

Fig. 2 Crystallinity degree of PA6 and PA6/CN at various cooling rates [7]

The value of heat of fusion, measured by DSC method, is commonly used to calculate the degree of crystallinity. In poly(ethylene oxide) (PEO)/organically modified MMT (OMMT) nanocomposites the degree of crystallinity continuously decreased with increasing clay content [2]. A decrease in the degree of crystallinity has been also reported to occur, i.e. in polyethylene [3], low density polyethylene (LDPE) [4], poly(vinylidene fluoride) [5] and polyamide-6 [6] nanocomposites reinforced with MMT or with bentonite clays. The DSC results also revealed an unusual phenomenon of an increase of crystallinity degree of PA6 nanocomposites with increasing cooling rate (Fig. 2) [7]. The DSC results show that the addition of a small amount of clay into the polymer results in an increase of crystallization temperature (T_c) of the polymer matrix; it can be explained by heterogeneous nucleation of polymer crystallization process induced by MMT. Such an effect was observed, for instance, in polypropylene grafted maleic anhydrite compolymer modified with hexamethylenediamine (designated as PP-*g*-HMA) matrix [8]. On the other hand, the nucleating ability of silicate layers was poor in PA-6 nanocomposites made by melt-extrusion because highly active, stable PA-6 crystallization precursors were generated during melt-extrusion [9]. Relatively small changes in T_c value were reported in nanocomposites of LDPE, too [4]. Opposite effect of shifting the temperature of crystallization to lower temperatures was observed for melt compounded poly(butylene terephthalate) (PBT) nanocomposites [10].

Kinetic analysis of the polymer crystallization gives further information about the effect of nanoparticles on mechanism of nucleation and crystals growth – it indicated an increase in the crystallization rate of polypropylene for low MMT contents as evidenced by half-crystallization time ($t_{1/2}$) [8]. It was lower (in comparison to pure polymers) for crystallization of numerous polymeric matrixes modified with OMMT [11–13].

The kinetic analysis of isothermal crystallization of polypropylene-grafted with maleic anhydride copolymer (PP-*g*-HMA) based nanocomposites showed significant changes of the Avrami exponent *n* that indicated the change of the crystal growth process from a three-dimensional crystal growth for pristine polymer to a two-dimensional spherulitic growth for nanocomposites. For PP-*g*-HMA sample, the *n* values were close to three within the range of analyzed crystallization temperatures (T_c) and might represent an athermal nucleation process, followed by a three-dimensional crystal growth. For nanocomposites the value of *n* ranged around 2.0–2.2 indicating that crystal growth may not occur in three dimensions at an equal rate [8]. Similarly, DSC isothermal results of syndiotactic polystyrene (sPS) nanocomposites containing 5 mass% of clay revealed strongly heterogeneous nucleation, inducing a change of the crystal growth process from mixed three-dimensional and two-dimensional crystal growth to two-dimensional spherulitic growth [14]. In extruded polyamide-6 (PA-6) nanocomposites with MMT, after a small initial increase in the overall crystallization rate at low MMT concentrations, the dispersed silicate layers decreased the overall PA-6 crystallization rate with a further increase of the MMT content [15]. At these higher concentrations, the silicate layers behaved as heterogeneities that retard the PA-6 crystal growth. Similarly, in poly(ε-caprolactone) very small amounts of clay dramatically increased the rate of crystallization [16]. However, high clay concentrations reduced the rate of crystallization. Complex crystallization behavior revealed also polylactide (PLA) nanocomposites [17]. For example, when the materials were crystallized from the melt in the temperature range from 120–130°C, the crystallization rate for the composite material was approximately 15 to 20 times faster than that for the neat PLA. The crystallization rate for the neat PLA was noted to increase with prolonged exposure (60 min) at 200°C, while the rate for the composite sample was noted to decrease. Wu *et al*. determined the activation energy for the transport of the poly(butylene terephthalate) (PBT) segments to the growing crystal surface by the Kissinger method [10]. The results indicated that the hybrids with small amounts of clay presented lower activation energy than pristine PBT, whereas those with higher clay loadings showed higher activation energy.

The kinetic analysis of the nanocomposites of syndiotactic 1,2-polybutadiene (sPB) revealed smaller Avrami exponent and larger crystallization rate constant, with respect to pristine sPB [18]. Primary crystallization under isothermal conditions displayed both

athermal nucleation and three-dimensional spherulite growth and under nonisothermal processes the mechanism of primary crystallization was found to be very complex. In the work of Causin *et al*. [19], the temperature of melting (T_{m0}) of the materials was calculated by the method proposed by Marand. The kinetics of crystallization was evaluated using Avrami model and the Hoffman–Lauritzen theory that connect chain folded crystal growth rate and undercooling. The interfacial free energy (σ_e), that may be estimated by the Hoffman–Lauritzen theory, is directly proportional to the work of chain folding and can then be used as a measure for evaluating how easy it is for macromolecules to fold into lamellae. Montmorillonite was found to depress T_{m0}, to enhance the rate of crystallization and to ease the chain folding of macromolecules. These effects were magnified if clay was exfoliated, rather than intercalated, so the role of the filler on the crystallization behavior was linked to the extent of the interfacial region between polymer and filler.

In another work the Avrami plots show that the crystal growth of PE in the intercalated sample is two-dimensional, while it is three-dimensional in the exfoliated sample. The crystallization activation energy of the intercalated sample is slightly smaller than that of the exfoliated sample [20].

The energy barrier of poly(ethylene-*co*-glycidyl methacrylate) (PEGMA) governing the non-isothermal melt-crystallization was evaluated according to Augis–Bennett model, Kissinger model and Takhor model [21]. Generally, the higher the activation energy (E) value, the lower the crystallization ability of the polymer becomes. The three models all showed that PEGMA/clay nanocomposite had a higher value of E than that of neat PEGMA, which indicated the nanocomposite had a lower crystallization rate.

DSC was also applied to study the influence of nanoparticles on the polymer matrix morphology formation. For instance, polymorphic behavior of PA-6 upon the addition of OMMT was studied [22–24]. On DSC heating scan, neat PA-6 is likely to show only one endothermic peak at temperature ($T_{m,\alpha}$) around 225°C, which was associated with the melting of α-form crystals [25–28]. In polymer modified with OMMT another endothermic peak, corresponding to the melting of the less stable γ-form crystals, was observed at temperature $T_{m,\gamma}$=ca. 215°C. OMMT was showed to enhance the formation of γ-form crystals in PA-6 matrix, especially when crystallization took place in lower temperature region. The most striking difference in melting behavior of PA-6/OMMT as compared to pure polymer was the occurrence of an additional melting peak at temperature higher than $T_{m,\alpha}$. The origin of the new peak was explained in terms of melting of specific lamellae fraction that was formed under stress in the volume of intercalated nanoclay sheets and tethered on the host layers by strong (interfacial) ionic interaction (Fig. 3). A superheating effect may have occurred as these constrained lamellae within the confined environment were heated in DSC experiment. New endothermic peak on DSC heating profiles was also observed for PA-6/OMMT nanocomposites that underwent crystallization under shear [29]. It was pointed that similar melting behavior was observed for PA-6 samples crystallized under pressure [30]. The influence of OMMT on crystalline forms was also observed in poly(vinylidene fluoride) (PVDF) nanocomposites [31]. The temperature of melting found by DSC analysis corresponded to the melting of the γ form that could be obtained in special conditions only and which is quite important since it exhibits piezo- and pyroelectric properties. Similar impact of nanolayers on crystalline phase morphology was observed in polyoxymethylene (POM) by DSC with temperature modulation (MT-DSC) [32]. Two endothermic peaks were observed on reversible heat flow profile of POM and POM/OMMT nanocomposites indicating the presence of two crystalline forms of polymer that underwent melting at different temperatures. The lower temperature melting peak was due to melting of extended chain crystals (ECC) followed by recrystallization, as evidenced by exothermic peak in reversible heat component course and finally, melting of folded chain crystals (FCC) was observed as higher temperature melting peak. The MT-DSC curves of

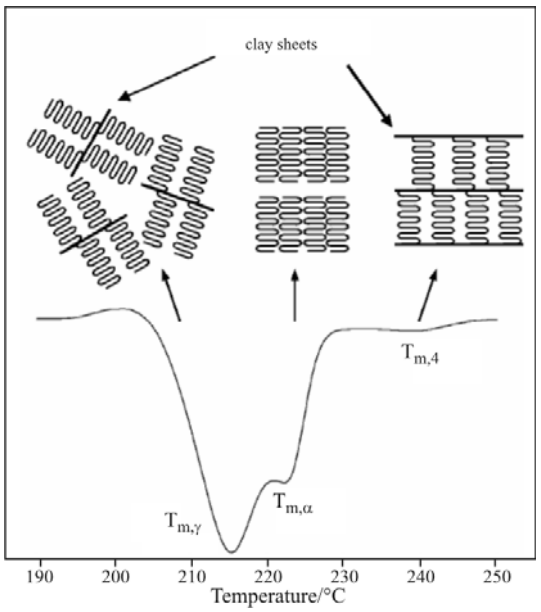

Fig. 3 Schematic model of the possible origin of the multiple melting peaks observed in the DSC study of the PA-6/OMMT nanocomposites [28]

nanocomposites evidenced strengthening and significant separation of the low temperature peak from the high temperature one. Montmorillonite seemed to favor the formation of extended chain crystals, especially under simultaneous shear imposed in injection molding. Similar morphology of POM was achieved by applying complex processing operations, e.g. biaxial stretching or melt spinning [33].

In other work the data derived from MTDSC showed the relationship between interlayer distance (Δd) and the increment of heat capacity (ΔC_p) for PU/clay intercalated nanocomposite [34]. For nanocomposites having small interlayer distances, smaller than the characteristic length ζa of bulk polyurethane (1.45 nm), the ΔC_p values were reduced. However, for clays 25A and 20A, the interlayer d-spacing was big enough for cooperatively rearranging of polyurethane molecular chain at dynamic glass transition, ΔC_p values remained the same as that of bulk polyurethane.

The DSC study on the curing process and its kinetics can give insight into the actual mechanism of cure reaction and its effect on degree of cross-linking and further on mechanical properties. DSC analysis of curing process of nitrile rubber (NBR)/layered clay nanocomposites showed a reduction in cure time and an increase in enthalpy of curing for the systems with organoclay; autocatalytic model showed the best fit in kinetic modelling [35]. There was a little change in the cure behavior of the NBR/unmodified clay system which suggested that the accelerating effect was due to introduction of ammonium modifier to MMT. Further, the cure kinetics studies on natural rubber–organoclay nanocomposites [36] and fluoroelastomer/organoclay nanocomposites [37] showed the suitability of the autocatalytic model for analyzing the cure parameters of rubber/clay nanocomposites. DSC analysis of cure kinetics of fluoroelastomer nanocomposites also confirmed the catalytic role of organomodifier on vulcanization process since opposite effect, consisting in slowing down the curing reaction, was observed in systems based on unmodified clay. It was ascribed to a cure retardation effect of Na-MMT by absorbing part of a curative. Moreover, in DSC experiments a catalytic effect of ammonium compounds on homopolymerization of epoxy resin was observed [38, 39]. In Seo *et al*. work an increase in curing rate with increasing clay content was considered to be due to the presence of OH groups of the organic modifier of the clay, which could accelerate the epoxy curing reactions [40].

Further, the DSC method is commonly applied to investigate the α-transition in polymers and their composites. The α-transition is related to the Brownian motion of the main chains at the transition from the glassy to the rubbery state and the relaxation of dipoles associated with it. DSC results showed an

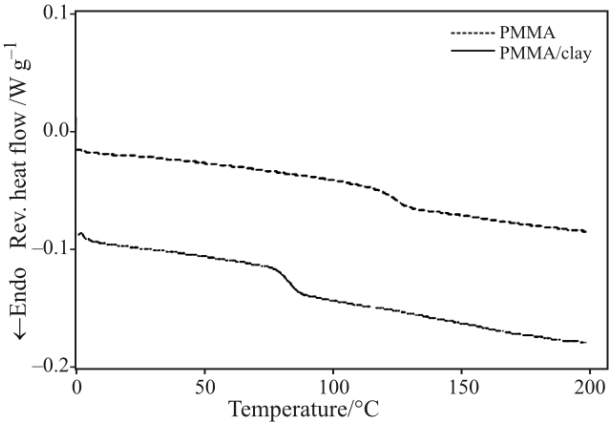

Fig. 4 DSC profiles of PMMA and PMMA/MMT nanocomposite [41]

increase in the glass transition temperature (T_g) of numerous polymers upon modification with montmorillonite, e.g. in poly(methyl methacrylate) (PMMA) [41], Fig. 4. This effect was typically ascribed to the confinement of intercalated polymer within the silicate galleries that prevents the segmental motions of the polymer chains. In the case of polyurethane-urea nanocomposites the changes of temperature of glass transition were also interpreted as a result of effective attachment of polymeric chains to the silicate surface [42]. It was pointed out that these anchored polymer chains could form an interphase region, where the segment relaxation was slower than in the bulk. The restricted relaxation behavior for the polymer nanocomposites with intercalated and exfoliated silicates depended primarily on the exfoliation extent of the layered silicates and the interaction strength between the silicate surfaces and the PU macromolecules. Interestingly, in poly(vinyl alcohol), that is a strongly polar polymer, the glass transition temperature (T_g) was completely disappeared, even at low levels of MMT clay loadings [43]. However, some nanocomposites (e.g. PLA/MMT) showed lowered glass transition temperatures [1], or there was no change in the glass transition temperature.

The glass transition temperature of sPS was reported to increase with MMT addition [44]. On the other hand, Bruzaud *et al*. found T_g of sPS nanocomposites almost unchanged and emphasized numerous factors influencing the glass transition process, such as the level of clay dispersion, different crystal structure of sPS homopolymer, as well as the nature of the interfacial sPS/clay grafted groups interactions. The work by Torre *et al*. indicated the influence of preparation route on the thermal properties of sPS nanocomposites [45]. A strong reduction in the T_g was observed only for composites

obtained from solution, whereas the composites obtained by melt intercalation showed T_g values approximately equal to that of pure polymer. However, some difficulties in detecting changes in T_g for polymer-clay nanocomposites may occur when using conventional DSC [46].

In Hutchinson's *et al*. work the DSC was used to estimate the influence of preparation method and conditions on thermal properties of epoxy-OMMT systems [47]. It was observed that DSC curves of pure epoxy resin and its nanocomposites differed slightly when the heat flow was calculated per gram of mixture of polymer and filler, but when it was calculated per g of resin (by dividing the curves for the resin/clay mixtures by resin content), then all the curves superposed to a very good approximation. This showed that both the glass transition temperature and the change in specific heat capacity, Δc_p, of the epoxy resin were not affected by the presence of the clay in the mixtures. Further, authors found two glass transitions of nanocomposite material that was prepared by solution method. The transitions were ascribed to bulk material and fraction of intercalated epoxy resin. Interestingly, from the Δc_p values for the two glass transitions an estimation of the relative proportions of bulk and intercalated resin was done. Thus the relative proportions of bulk resin and intercalated resin estimated in this way were 90.9 and 9.1%, respectively. The reduction of Δc_p of nanocomposites was reported elsewhere [48, 49]. However, by use of MT-DSC method it was shown that reduction Δc_p is more likely to occur in nanocomposites containing high clay content [50].

Kinetic analysis of the glass transition of polymer-clay nanocomposites may provide mechanistic clues into pathways of how MMT influences this thermally activated process in polymer.

The application of the isoconversional method to the resulting conversion (α) *vs*. temperature (T) data obtained from DSC measurements at different heating rates allows one to determine a variation of activation energy (E) with the extent conversion (α) from the glassy to rubbery state. Basing on DSC measurements, Vyazovkin *et al.* demonstrated that the activation energies for the glass transition in PS/clay nanocomposites were markedly greater than in pure PS throughout the glass transition region [51].

Calorimetric experiments at cooling rates comparable to those during e.g. injection molding are needed to study phase transitions under conditions relevant to processing. Ultra fast scanning calorimetry is a technique which provides a means to analyze the crystallization behavior of nanocomposite systems containing fast crystallizing polymers [52]. No influence of clay loading was observed by using this technique at lower crystallization temperatures of isotactic polypropylene (iPP) [53]. At these temperatures, where the mesophase is formed and homogeneous nucleation is expected, the contribution of the clay as a nucleating agent was negligible. For crystallization at about 80°C, where the α-phase is formed, the nucleating effect of the clay was observed yielding complex crystallization kinetics. In the temperature range of 75–85°C in some nanocomposites a double peak during isothermal crystallization was observed which originates from crystallization processes of different rate occurring simultaneously. At higher temperatures, above 120°C, the clay slightly retarded the crystallization process.

Dynamic mechanical thermal analysis

One of the basic ideas of modifying polymers with nanoplates of clays is to enhance the material's mechanical properties. DMA was frequently used in nanocomposites characterization since it allows the measurement of two different moduli of the nanocomposites, a storage modulus (E') which is related to the ability of the material to return or store mechanical energy and a loss modulus (E") which is related to the ability of the material to dissipate energy as a function of temperature. DMA data show significant improvements in the storage modulus over a wide temperature range of a number of polymer nanocomposites with MMT, such as PVDF [31], PP [54] and PMMA [55].

In nanocomposites of PA-6 a linear increase of storage modulus with increasing clay content was observed with a simultaneous decrease in intensity of main relaxation peak [56]. The linear changes of modulus in the temperatures below T_g were in accordance with parallel coupling model, since in glass state both the amorphous and crystal phases of PA-6 have similar mechanical properties. Above the glass transition temperature the amorphous phase become rubbery and the storage modulus changes from about 1 GPa to 1 MPa.

The improvement of thermomechanical properties of nanocomposites may be explained in terms of restricted thermal motions of polymer enveloped by clay nanoplates. The orientation of nanoparticles and higher-order structures of polymer influences the thermomechanicl properties as well. Apart from polymer morphology, the strength of interphase interactions was shown to be an important factor [57]. Introduction of a macromolecular compatibilizer in order to improve the interphase properties and facilitate the exfoliation of OMMT was beneficial in terms of thermomechanical properties.

The DMA method is commonly used to determine the glass transition temperature of polymeric materials from the peak of loss angle tangent (tgσ).

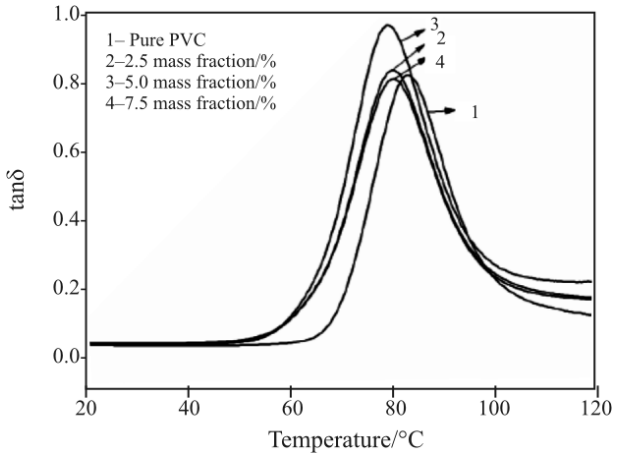

Fig. 5 Variation of tanó with temperature for PVC and PVC/MMT nanocomposites with different loading of OMMT [58]

In the PVC/MMT composites decrease in T_g was reported (Fig. 5) [58]. The T_g lowering was caused by exfoliated MMT layers dispersed in PVC matrix at nano-sized scale that keep PVC macromolecules apart and decrease the intermolecular interaction between PVC macromolecules in nanocomposites with MMT. In Masenelli-Varlot *et al*. work the DMA analysis showed a downshift of the glass temperature that was assigned to the plasticizing effect caused by surfactant used for MMT modification [56]. It was also noted that the changes of glass transition temperature determined from the peak of loss factor (tgσ) may reflect the way the various system components are sharing the deformation energy provided to the whole composite structure. A combination of factors was pointed as probable cause of T_g decrease in epoxy resins based on diglycidyl ether of bisphenol-A (DGEBA), such as catalytic effect of MMT towards homopolymerization reaction, unreacted resin plasticization and lower crosslinking density [59]. In the case of iPP–clay nanocomposites the turning point of relaxation behavior appeared at organoclay content of 1 mass% [60]. Before this point, the effect of organoclay can be negligible and the increase of chain mobility was ascribed to the decrease of molecular mass of polymer chains, as commonly occurs during dynamic melt processing; after this point, however, a reduced mobility of chains and a retarded chain relaxation were observed and attributed to the formation of a mesoscopic filler network. It was identified that the impact of nanodispersed OMMT tactoids and layers on the mobility of iPP chains is weak before the construction of a percolated filler network. One may postulate that the percolated filler network induces cooperative motion of iPP chains through the conjunction of OMMT sheets with iPP chains, resulting in retarded relaxation of the oriented structure and improved structural reversibility of iPP/OMMT.

However, kinetic analysis of glass transition and evaluation of activation energy is more informative on relaxation behaviour of polymers upon modification of MMT that only T_g measurements. Vyazovkin *et al*. determined energy of activation of glass transition from DMA runs [51]. The temperatures of the peaks, T_p, have been determined at five different frequencies, f, and the plots of $\ln f$ *vs*. T_p^{-1} showing good linearity allowed to calculate the activation energy of glass transition (360 kJ mol^{-1} for PS and 540 kJ mol^{-1} for PS–clay nanocomposite). The obtained relaxation data indicated that the long chain molecular motion in the PS–clay nanocomposite encountered a markedly larger energy barrier than in virgin PS. This implies that at the same temperature the nanocomposite should have lower molecular mobility than the virgin polymer. It was noticed that the changes in molecular mobility, which is claimed to be the major factor contributing to the transport of reactive species (e.g., oxygen and/or radicals) within the polymer, may explain the lower reactivity of nanocomposite and, therefore, its greater chemical and thermal stability as compared to virgin PS.

By using DMA it was also found that constraining some of the polymer chains reduces the magnitude of the loss response in the material [61]. When the constrained regions surrounding the filler particles are large enough to overlap, a second glass transition can be identified as a small, higher temperature, α' relaxation in the loss tangent trace. This secondary, α', transition may be the glass transition of the nylon-6 chains in the constrained region, as explained by Eisenberg and Tsagaropoulos [62], or in the crystalline region, as explained by Takayanagi [63].

Apart from the main relaxation temperature (α-relaxation) also the temperatures of secondary relaxation (β-relaxation) of nanocomposites were determined by using DMA. Secondary relaxation is a process that has been reported to be related to some unspecified local non-cooperative mobility occurring in the sub-T_g temperature region [64]. However, there is no single accepted view of what β-relaxation process is. It was found that the presence of organoclay steadily decreased β-relaxation temperatures with increasing filler concentration in epoxy resins [59]. There β-relaxation is related to crankshaft rotation of the hydroxy ether segments (–CH_2–CH(OH)–CH_2–O–) of the crosslinked network in the glassy state. That changes generally followed the behavior of nanocomposite material in the region of glass transitions. Similar observations concerning β-relaxation were reported for PVC polymeric systems [65]. The lowering temperature of tran-

sition was accompanied by broadening of relative peak on the loss tangent curve (tgσ). The influence of MMT on the relaxation behavior of PVC chains was explained in terms of confinement of polymer chains depending on the extent of nanoparticles dispersion. In the case of poly(vinyl alcohol) no influence of clay on relaxation behavior of polymer was found in the region of β- and γ-relaxation as stated from both dynamic mechanical thermal analysis and dielectric spectroscopy [66].

Thermal mechanical analysis

TMA is a highly sensitive method for the measurement of expansion and contraction of cross-linked or filled materials, including nanocomposites [67]. TMA was used to measure the coefficient of thermal expansion (CTE) of nanocomposite materials based on PA-6 [68], PP [67], PA [69] – it has been found that CTE is lower in nanomaterials in comparison to unmodified polymer, especially for low contents of OMMT. PA-6 modified with OMMT exhibited lower values of CTE than pure polymer in the direction parallel to the melt flow during injection molding [68], while increased values of CTE were measured in the direction normal to the melt flow. TMA results may indirectly provide information about the spatial orientation of MMT layers in nanocomposite material.

Thermogravimeric analysis

The literature concerning thermal stability and degradation of polymer/clay nanocomposites covers numerous original papers as well as comprehensive review articles [70–73]. Introduction of montmorillonite into polymer matrix was commonly used to improve thermal stability of polymer. However, the effect of nanofiller on the thermal stability of polymer depends on numerous factors including chemical constitution of surfactant molecule [41, 74], structure of nanocomposite material [75], the degree of MMT dispersion [76, 77], as well as the method and conditions of nanocomposite preparation [78, 79].

The critical parameter for thermal stability improvement is the stability of organic compound used to modify interfacial properties of montmorillonite. Since the onset temperature of degradation of commonly used ammonium organomodifier is close to processing temperatures of most large-scale produced polymers their decomposition may proceed during fabrication of nanocomposite. As a result, limited degree of MMT dispersion is achieved and contamination the polymer matrix with products of thermal decomposition may take place. For instance, after homogenization of OMMT in polyimide matrix the interlayer distance of clay was diminished instead of increased [80]. Similar effect was observed during preparation of PA-6 nanocomposites [81]. Other disadvantageous effect was reported by Tidjani *et al*. and was connected with the presence of reactive hydroxyl group in organofilizer molecule that produced reactive species accelerating degradation of polymer upon heating [82].

The investigations of thermal stability of poly(ε-caprolactone) (PCL) by means of thermogravimetry showed that thermal resistance of exfoliated nanocomposite was superior to intercalated one and the microcomposites underwent degradation in the lowest temperature range. In the case of PCL nanocomposites the higher was the area of interphase contact the higher was the thermal stability [83].

TG analysis of polyurethane/OMMT nanocomposites showed the highest thermal stability for 1 mass% content of OMMT since this system was characterized by the highest dispersion and therefore the highest area of interphase contact [84]. Interestingly, the thermal stability of polycarbonate (PC) nanocomposite decreased with increasing dispersion degree of OMMT [85]. Degradation of PC was accelerated by OMMT or products of its degradation since polymer exhibited yellowing and reduction of molecular mass under contact with MMT. Nevertheless, the modification was beneficial in terms of fire resistance. Generally, the degradation of alkylammonium cation intercalated into montmorillonite layers is believed to follow the Hoffman's elimination mechanism that involve the formation of unsaturated hydrocarbon (an olefin), amine and acidic proton which is left on the surface of MMT [86]. The presence of the acidic sites is believed to produce catalytic effect on the initial stage of polymer degradation process resulted in a shift of initial temperature of degradation towards lower temperature region. This phenomena was observed in PVC [87], PA-6 [88] and PP [89].

The results of kinetic analysis of degradation process can be considered in terms of energy barriers as well as offer an insight into the mechanisms of thermal stability improvement. The isoconversional methods such as the methods of Friedman [90], Ozawa [91] and Flynn and Wall [92] as well as method advanced by Vyazovkin [93, 94], require performing a series of experiments at different temperature programs and yield the values of effective activation energy as a function of conversion.

Kinetic analysis applying advanced isoconversional method demonstrated a markedly larger effective activation energy of the whole process of PS–clay nanocomposites degradation and showed an increase in effective activation energy of nanocomposite at lower conversion comparing to pure PS [51, 95]. That increase most likely represents a shift of the limiting

step from initiation at the weak links to random scission. The total increase in activation energy of a process seemed not to support the barrier model of thermal stability improvement that assumes the degradation rate of a polymer–clay nanocomposite should be limited by the diffusion of gaseous decomposition products through the surface barrier of the silicate char. It was argued that the diffusion of gases in liquids and solids, including polymers, tends to have a low activation energy of about 40–50 kJ mol^{-1}. The accuracy of the barrier model in relation to investigated PS–clay nanocomposites was questioned since the DSC results of nanocomposites showed significant (30%) decrease in endothermic effect observed during pyrolytic degradation and about three times larger endothermic effect in air than the respective effects observed for pure PS. This effects are not likely to result from only the presence of the surface barrier and suggested rather that the introduction of the clay phase in PS changed the concentration distribution of degradation products and/or might cause the formation of some new products of degradation. The later assumption was further confirmed by application of thermoanalytical methods that showed the increased intensity of evolution of α-methylstyrene in addition to styrene monomer, dimer and trimer typically observed in degradation of pure PS. Because a-methylstyrene is a product of interchain hydrogen transfer, its formation was readily explained by nanoconfinement of PS chains estimated as a decrease in the average interchain distance from 8.2 nm in virgin PS to 3.8 nm in the PS–clay brush system [96].

Bourbigot *et al*. have used isoconversional method to analyse the kinetic of thermal and thermooxidative degradation of PS–clay nanocomposites [97]. A model-free Friedman analysis, provided the plot of the activation energy *vs*. the fractional mass loss that was informative whether the degradation goes through one-step reaction or multistep reactions take place. Further, the modeling of degradation process of pure polymer and its nanocomposites was applied in order to indicate the most probable global kinetic model of reactions. It was found e.g. for PS thermal degradation that the best fit quality of experimental data had two competitive reactions. Random scission of the polymeric chains was assigned to first reaction and end-chain and mid-chain β-scission, radical recombination and hydrogen transfer for the second reaction. The work brought to conclusion that the probability of end-chain and mid-chain β-scission, radical recombination and hydrogen transfer reactions might be decreased in PS nanocomposite during pyrolytic degradation. In the route of thermooxidative degradation of PS–clay nanocomposites four main model reactions were described: reaction (1) oxygen initiated depolymerization of PS (the presence of the clay in PS lowered the energy of this reaction), reaction (3) in competition with reaction (1) (the higher activation energy and higher char masses of nanocomposite material suggested that the clay played the role of char promoter), reactions (2) and (4) corresponding to char oxidation (the activation energies of reactions (2 and 4) of nanocomposite compared to pure PS were similar suggesting the same type of reaction of oxidation).

The detailed mechanism of improvement of nanocomposite thermal stability has not been well established yet and the results indicate complex influence of nanofiller on physical and chemical processes running during thermal degradation of polymer. The common opinion is that the improvement in thermal stability of nanocomposites is due to the formation of char on the nanocomposite surface that is enhanced by impermeable MMT layers [98–100]. This char reduces the diffusion of volatile products of polymer degradation out of polymer bulk; therefore the reduction in the rate of mass loss is observed. The introduction of anisometric impermeable nanoparticles into polymer results in formation of labyrinth in bulk of material that volatile products must escape. This effect also reduces the diffusion of atmospheric oxygen into material during thermooxidative degradation [101]. The role of montmorillonite as thermal insulating material that reduces the heat transport in nanocomposite matrix is also indicated to contribute to thermal stability improvement [102]. The same MMT feature may lead to accumulation of thermal energy in nanocomposite material and degradation of polymer in superheated conditions.

The mechanism of thermal stability improvement was also ascribed to the changes in the dynamics of polymer molecular motion [103]. This effect involves the reduction of transport of reactive species in nanocomposite and causes changes in kinetics of chemical reactions proceeding during thermal decomposition of polymer. Moreover, in a more recent work [104], it was shown that the formation of char occurs in later stages of degradation as a result of migration of nanoparticles towards the composite surface driven by changes in the surface free energy [105]. On the other hand, changes in mechanism of PS degradation proved by variation of kinetic parameters, total heat of degradation and evolution of new products [104], as well as improved thermal stability of non-char-forming polymers (e.g. [106]), implies the (co)existence of other mechanism that especially controls the initial step of thermal degradation.

Therefore, changes in kinetics of degradation as well as dynamic properties of nanocomposite materials resulted from nanoconfinement of polymer may account for the mechanism of thermal stability

improvement. Nanoconfinement can be invoked as a mechanism that explains change in course of other thermally stimulated processes in polymer–clay nanocomposites such as glass transition dynamics and related intermolecular cooperativity of the polymer matrix. For example, the size of cooperatively rearranging region (CRR) in PS–clay nanocomposites estimated from the data on the quasi-static heat capacity, $C_{p,0}$ according to Donth's equation [107] increased significantly in the exfoliated brush material, making individual motions of macromolecules more mutually dependent and did not practically change in the intercalated system [104]. That indicated an important difference in the structure of the bulk polymer in the respective nanoconfined environments. Therefore, this parameter was pointed as a useful tool in characterizing the structure of nanoconfinement. The invariability of its value for a nanocomposite as compared to that for a regular nonconfined polymer matrix indicates that nanoconfinement is localized at the clay particles. However, a significant increase in the size of cooperatively rearranging region suggests that nanoconfinement is more delocalized throughout the polymer matrix. It was speculated that in nanoconfined environments of polymer–clay grafted nanocomposites where the clay sheets anchor several polymer chains, the probability of intermolecular reactions is higher and favours the formation of new product of degradation as a result of changing a branching ratio of the individual channels [96]. The evolution of new products of degradation was observed by thermogravimetry coupled with mass spectrometry (TG-MS) or infrared spectroscopy (TG-FTIR) [108–112]. The results enabled to propose the mechanism of thermal stability improvement of polymeric nanocomposites based on different polymers in terms of radical stability. The simultaneous heat and barrier effect of MMT may enhance the secondary reactions of relatively stable radicals, such as recombination or cyclization and formation of less volatile compounds. New formed products may further contribute to char formation and enhance thermal resistance of polymer.

Conclusions

The results of thermal analysis show that the presence of montmorillonite in polymer matrix implies modifications on physical and chemical processes, such as melting-crystallization transitions, structural relaxation phenomena and kinetics of reactions that proceed during nanocomposite synthesis (polymerization) or degradation. Thermal analysis offers a wide range of techniques that were used to determine the properties of polymeric nanocomposites and to expand the knowledge on the mechanisms of thermal properties improvement. Apart from the scientific value, wide investigations on thermal properties of polymeric nanocomposites based on layered silicates contribute to technology development and production of advanced polymeric material with desired structure, morphology and properties.

References

1 H. Tian and H. Tagaya, J. Mater. Sci., 42 (2007) 3244.
2 M. Y. Hikosaka, S. H. Pulcinelli, C. V. Santilli, K. Dahmouche and A. F. Craievich, J. Non-Cryst. Solids, 352 (2006) 3705.
3 T.G. Gopakumar, J.A. Lee, M. Kontopoulou and J. S. Parent, Polymer 43 (2002) 5483.
4 J. Morawiec, A. Pawlak, M. Slouf, A. Galeski, E. Piorkowska and N. Krasnikowa, Eur. Polym. J., 41 (2005) 1115.
5 L. Priya and J.P. Jog, J. Polym. Sci., Part B: Polym. Phys., 40 (2002) 1682.
6 S. C. Tjong and S. P. Bao, J. Polym. Sci., Part B: Polym. Phys., 42 (2004) 2878.
7 X. Liu and Q. Wu, Eur. Polym. J., 38 (2002) 1383.
8 J.-Y. Wu, T.-M. Wu, W.-Y. Chen, S.-J. Tsai, W.-F. Kuo and G.-Y. Chang, J. Polym. Sci.: Part B: Polym. Phys., 43 (2005) 3242.
9 D. S. Homminga, B. Goderis, V. B. F. Mathot and G. Groeninckx, Polymer, 47 (2006) 1630.
10 D. Wu, C. Zhou, X. Fan, D. Mao and Z. Bia, J. Appl. Polym. Sci., 99 (2006) 3257
11 W. B. Xu, H. B. Zhai, H. Y. Guo, Z. F. Zhou, N. Whitely and W.-P. Pan, J. Therm. Anal. Cal., 78 (2004) 101.
12 Y. Wang, C. Shen, H. Li, Q. Li and J. Chen, J. Appl. Polym. Sci., 91 (2004) 308.
13 C. I. W. Calcagno, C. M. Mariani, S. R. Teixeira and R. S. Mauler, Polymer, 48 (2007) 966.
14 T.-M. Wu, S.-F. Hsu, C.-F. Chien and J.-Y. Wu, Polym. Eng. Sci., 44 (2004) 2288.
15 T. D. Fornes and D. R. Paul, Polymer, 44 (2003) 3945.
16 G. Jimenez, N. Ogata, H. Kawai and T. Ogihara, J. Appl. Polym. Sci., 64 (1997) 2211.
17 M. Day, A. Victoria Nawaby and X. Liao, J. Therm. Anal. Cal., 86 (2006) 623.
18 J. Cai, Q. Yu, Y. Han, X. Zhang and L. Jiang, Eur. Polym. J., 43 (2007) 2866.
19 V. Causin, C. Marega, R. Saini, A. Marigo and G. Ferrara, J. Therm. Anal. Cal., 90 (2007) 849.
20 J.-T. Xu, Q. Wang and Z.-Q. Fan, Eur. Polym. J., 41 (2005) 3011.
21 J.-W. Huang, H.-C. Hung, K.-S. Tseng and C.-C. Kang, J. Appl. Polym. Sci., 100 (2006) 1335.
22 F.-C. Chiu, S.-M. Lai, Y.-L. Chen and T.-H. Lee, Polymer, 46 (2005) 11600.
23 T. M. Wu, E. C. Chen and C. S. Liao, Polym. Eng. Sci., 42 (2002) 1141.
24 I. González, J. I. Eguiazábal and J. Nazábal, Compos. Sci. Technol., 66 (2006) 1833.
25 L. M. Liu, Z. N. Qi and X. G. Zhu, J. Appl. Polym. Sci., 71 (1999) 1133.

26 T. M. Wu and C. S. Liao, Macromol. Chem. Phys., 201 (2000) 2820.
27 K. Varlot, E. Reynaud, M.H. Kloppfer, G. Vigier and J. Varlet, J. Polym. Sci., Part B: Polym. Phys., 39 (2001) 1360.
28 T.-C. Li, J. Ma, M. Wang, W. C. Tjiu, T. Liu and W. Huang, J. Appl. Polym. Sci., 103 (2007) 1191.
29 F. J. Medellin-Rodriguez, C. Burger, B. S. Hsiao, B. Chu, R. Vaia and S. Phillips, Polymer, 42 (2001) 9015.
30 Y. Kojima, T. Matzuoka, H. Takahashi and T. Kuaruchi, J. Appl. Polym. Sci., 51 (1994) 683.
31 L. Priya and J. P. Jog, J. Polym. Sci., Part B: Polym. Phys., 41 (2003) 31.
32 A. Leszczynska and K. Pielichowski, in preparation.
33 J. M. Samon, J. M. Schultz, B. S. Hsiao, S. Khot and H. R. Johnson, Polymer, 42 (2001) 1547.
34 H. Xia and M. Song, Thermochim. Acta, 429 (2005) 1.
35 D. Choi, M. A. Kader, B.-H. Cho, Y. Huh and C. Nah, J. Appl. Polym. Sci., 98 (2005) 1688.
36 M. A. López-Manchado, M. Arroyo, B. Herrero and J. Biagiotti, J. Appl. Polym. Sci., 89 (2003) 1.
37 M. A. Kader and C. Nah, Polymer, 45 (2004) 2237.
38 T. Lan, P. D. Kaviratna and T. J. Pinnavaia, J. Phys., Chem. Sol., 57 (1996) 1005.
39 M.-T. Ton-That, T.-D. Ngo, P. Ding, G. Fang, K. C. Cole and S. V. Hoa, Polym. Eng. Sci., 44 (2004) 1132.
40 K. S. Seo and S. K. Dae, Polym. Eng. Sci., 46 (2006) 1318.
41 W. Xie, Z. Gao, K. Liu, W.-P. Pan, R. Vaia, D. Hunter and A. Singh, Thermochim. Acta, 339 (2001) 367.
42 B. Sreedhar, D. K. Chattopadhyay and V. Swapna, J. Appl. Polym. Sci., 100 (2006) 2393.
43 S. G. Abd Alla, H. M. Nizam El-Din and A. M. El-Naggar, J. Appl. Polym. Sci., 102 (2006) 1129.
44 C. I. Park, W. M. Choi, M. H. Kim and O. O. Park, J. Polym. Sci., Part B: Polym. Phys., 42 (2004) 1685.
45 L. Torre, G. Lelli and J. M. Kenny, J. Appl. Polym. Sci., 100 (2006) 4957.
46 E. Verdonck, K. Schaap and L.C. Thomas, Int. J. Pharm., 192 (1999) 3.
47 J. M. Hutchinson, S. Montserrat, F. Román, P. Cortés and L. Campos, J. Appl. Polym. Sci., 102 (2006) 3751.
48 R. Krishnamoorti, R. A. Vaia and E. P. Giannelis, Chem. Mater., 8 (1996) 1728
49 Y. Li and H. Ishida, Macromolecules, 38 (2005) 6513.
50 N. N. Bhiwankar and R. A. Weiss, Polymer, 47 (2006) 6684.
51 S. Vyazovkin, I. Dranca, X. Fan and R. Advincula, J. Phys., Chem. B, 108 (2004) 11672.
52 K. Pielichowski and K. Flejtuch, Polimery, 49 (2004).
53 V. V. Ray, A. K. Banthia and C. Schick, Polymer, 48 (2007) 2404
54 S. G. Lei, S. V. Hoa and M.-T. Ton-That, Compos. Sci. Technol., 66 (2006) 1274.
55 P. Meneghetti and S. Qutubuddin, Thermochim. Acta, 442 (2006) 74.
56 K. Masenelli-Varlot, E. Reynaud, G. Vigier and J. Varlet, J. Polym. Sci.: Part B: Polym. Physics, 40 (2002) 272.
57 X. Liu, Q. Wu, L. A. Berglund, H. Lindberg, J. Fan and Z. Qi, J. Appl. Polym. Sci., 88 (2003) 953.
58 D.-Y. Yang, Q.-X. Liu, X.-L. Xie and F.-D. Zeng, J. Therm. Anal. Cal., 84 (2006) 355.
59 O. Becker, R. Varley, G. Simon, Polymer, 43 (2002) 4365.
60 K. Wang, S. Liang, J. Deng, H. Yang, Q. Zhang, Q. Fu, X. Dong, D. Wang and C. C. Han, Polymer, 47 (2006) 7131.
61 J. S. Shelley, P. T. Mather and K. L. Devries, Polymer, 42 (2001) 5849.
62 G. Tsagaropoulos and A. Eisenberg, Macromolecules, 28 (1995) 6067.
63 M. Takayanagi, Mem. Fac. Eng., 23 (1963) 80.
64 S. Vyazovkin and I. Dranca, Thermochim. Acta, 446 (2006) 140.
65 C. Wan, X. Qiao, Y. Zhang and Y. Zhang, Polym. Test., 22 (2003) 453.
66 I. Cendoya, D. López, A. Alegriá and C. Mijangos, J. Polym. Sci.: Part B: Polym. Phys., 39 (2001) 1968.
67 H. Krump, A. S. Luyt and I. Hudec, Mater. Lett., 60 (2006) 2877.
68 P. J. Yoon, T. D. Fornes and D. R. Paul, Polymer, 43 (2002) 6727.
69 Z.-M. Liang, J. Yin, J.-H. Wu, Z.-X. Qiu and F.-F. He, Eur. Polym., J. 40 (2004) 307.
70 A. Leszczynska, J. Njuguna, K. Pielichowski and J. R. Banerjee, Thermochim. Acta, 453 (2007) 75.
71 A. Leszczynska, J. Njuguna, K. Pielichowski and J. R. Banerjee, Thermochim. Acta, 454 (2007) 1.
72 J. K. Pandey, K. R. Reddy, A. P. Kumar and R. P. Singh, Polym. Degrad. Stab., 88 (2005) 234.
73 K. Pielichowski and A. Leszczynska, Polimery, 51 (2006) 60.
74 E. M. Araújo, R. Barbosa, C. R. S. Morais, L. E. B. Soledade, A. G. Souza and M. Q. Vieira, J. Therm. Anal. Cal., 90 (2007) 841.
75 J. Wang, Y. Chen and J. Wang, J. Appl. Polym. Sci., 99 (2006) 3578.
76 S. K. Srivastava, M. Pramanik and H. Acharya, J. Polym. Sci.: Part B: Polym. Phys., 44 (2006) 471.
77 A. Riva, M. Zanetti, M. Braglia, G. Camino and L. Falquic, Polym. Degrad. Stab., 77 (2002) 299.
78 X. Zheng and C. A. Wilkie, Polym. Degrad. Stab., 82 (2003) 441.
79 G. Chigwada, D. Wang and C. A. Wilkie, Polym. Degrad. Stab., 91 (2006) 848.
80 D. M. Delozier, R. A. Orwoll, J. F. Cahoon, N. J. Johnston, J. G. Smith Jr. and J. W. Connell, Polymer, 43 (2002) 813.
81 R. K. Shah and D. R. Paul, Polymer, 45 (2004) 2991.
82 A. Tidjani, O. Wald, M.-M. Pohl, M. P. Hentschel and B. Schartel, Polym. Degrad. Stab., 82 (2003) 133.
83 B. Lepoittevin, N. Pantoustier, M. Devalckenaere, M. Alexandre, D. Kubies, C. Calberg, R. Jérôme and P. Dubois, Macromolecules, 35 (2002) 8385.
84 Y. I. Tien and K. H. Wei, J. Appl. Polym. Sci., 86 (2002) 1741.
85 H. A. Stretz, J. H. Koo, V. M. Dimas and Y. Zhang, Polym. Prepr., 42 (2001) 50.
86 W. Xie, Z. M. Gao, W. P. Pan, D. Hunter, A. Singh and R. A. Vaia, Chem. Mater., 13 (2001) 2979.
87 T. Ren, J. Yang, Y. Huang, J. Ren and Y. Liu, Polym. Compos., 27 (2006) 55.
88 H. Qin, Q. Su, S. Zhang, B. Zhao and M. Yang, Polymer, 44 (2003) 7533.
89 Y. Tang, Y. Hu, L. Song, R. Zong, Z. Gui, Z. Chen and W. Fan, Polym. Degrad. Stab., 82 (2003) 127.
90 H. Friedman, J. Polym. Sci. C, 6 (1964) 183.
91 T. Ozawa, Bull. Chem. Soc. Jpn., 38 (1965) 1881.

92 H. Flynn and L. A. Wall, J. Res. Natl. Bur. Stand., 70A (1966) 487.
93 S. Vyazovkin and D. Dollimore, J. Chem. Inf. Comp. Sci., 36 (1996) 42.
94 S. Vyazovkin, J. Comput. Chem., 22 (2001) 178.
95 S. Vyazovkin, I. Dranca, X. Fan and R. Advincula, Macromol. Rapid Commun., 25 (2004) 498.
96 K. Chen, M. A. Susner and S. Vyazovkin, Macromol. Rapid Commun., 26 (2005) 690.
97 S. Bourbigot, J. W. Gilman and C. A. Wilkie, Polym. Degrad. Stab., 84 (2004) 483.
98 J. Zhu, A. B. Morgan, F. J. Lamelas and C. A. Wilkie, Chem. Mater., 13 (2001) 3774.
99 J. W. Gilman, Appl. Clay Sci., 15 (1999) 31.
100 M. Alexandre and P. Dubois, Mater. Sci. Eng., 28 (2000) 1.
101 M. Zanetti, G. Camino, R. Thomann and R. Mülhaupt, Polymer, 42 (2001) 4501.
102 H. A. Stretz, M. W. Wootan, P. E. Cassidy and J. H. Koo, Polym. Adv. Technol., 16 (2005) 239.
103 S. Vyazovkin and I. Dranca, J. Phys., Chem. B, 108 (2004) 11981.
104 K. Chen, C. A. Wilkie and S. Vyazovkin, J. Phys. Chem. B, 111 (2007) 12685.
105 M. Lewin, Fire Mater., 27 (2003) 1.
106 M. Zanetti, P. Bracco and L. Costa, Polym. Degrad. Stab., 85 (2004) 657.
107 E. Donth, J. Polym. Sci. B: Polym. Phys., 34 (1996) 2881.
108 B. N. Jang, M. Costache and C. A. Wilkie, Polymer, 46 (2005) 10678.
109 B. N. Jang and C. A. Wilkie, Polymer, 46 (2005) 3264.
110 M. C. Costache, D. Wang, M. J. Heidecker, E. Manias and C. A. Wilkie, Polym. Adv. Technol., 17 (2006) 272.
111 S. Su, D. D. Jiang and C. A. Wilkie, Polym. Degrad. Stab., 84 (2004) 269.
112 J. M. Hwu, G. J. Jiang, Z. M. Gao, W. Xie and W. P. Pan, J. Appl. Polym. Sci., 83 (2002) 1702.

DOI: 10.1007/s10973-008-9128-6